

# Composite spin and quadrupole wave in the ordered phase of $\text{Tb}_{2+x}\text{Ti}_{2-x}\text{O}_{7+y}$

H. Kadowaki, H. Takatsu, and T. Taniguchi

*Department of Physics, Tokyo Metropolitan University, Hachioji-shi, Tokyo 192-0397, Japan*

B. Fåk and J. Ollivier

*Institute Laue Langevin, BP156, F-38042 Grenoble, France*

(Dated: July 2, 2021)

The hidden ordered state of the frustrated pyrochlore oxide  $\text{Tb}_{2+x}\text{Ti}_{2-x}\text{O}_{7+y}$  is possibly one of the two electric multipolar, or quadrupolar, states of the effective pseudospin-1/2 Hamiltonian derived from crystal-field ground state doublets of non-Kramers  $\text{Tb}^{3+}$  ions. These long-range orders are antiparallel or parallel alignments of transverse pseudospin components representing electric quadrupole moments, which cannot be observed as magnetic Bragg reflections by neutron scattering. However pseudospin waves of these states are composite waves of the magnetic-dipole and electric-quadrupole moments, and can be partly observed by inelastic magnetic neutron scattering. We calculate these spin-quadrupole waves using linear spin-wave theory and discuss previously observed low-energy magnetic excitation spectra of a polycrystalline sample with  $x = 0.005$  ( $T_c = 0.5$  K).

## I. INTRODUCTION

Geometrically frustrated magnets have been actively studied in recent years [1]. In particular, pyrochlore magnets [2] showing spin ice behavior [3] have interesting features such as finite zero-point entropy and emergent magnetic monopole excitations [4]. A quantum spin-liquid state is theoretically predicted for certain spin-ice like systems [5–9], where transverse spin interactions transform the classical spin ice into quantum spin liquid. This quantum spin ice (QSI), or U(1) quantum spin liquid, is characterized by an emergent U(1) gauge field fluctuating down to  $T = 0$  and by excitations of gapped bosonic spinons and gapless photons [5, 7, 10]. By changing the interactions of the QSI in some ways the system undergoes a quantum phase transition to long range ordered (LRO) states of transverse spin or pseudospin [6], being interpreted as Higgs phases [7, 11]. Experimental investigations of the U(1) quantum spin liquid and neighboring LRO states have been challenged by several groups [9, 11, 12]. However it is difficult to characterize the quantum spin liquid states, which preclude standard techniques of observing magnetic Bragg reflections and magnons.

Among magnetic pyrochlore oxides [2],  $\text{R}_2\text{Ti}_2\text{O}_7$  ( $\text{R} = \text{Dy}, \text{Ho}$ ) are the well-known classical Ising spin-ice examples [3]. A similar system  $\text{Tb}_2\text{Ti}_2\text{O}_7$  (TTO) has attracted much attention, because magnetic moments remain dynamic with short range correlations down to 50 mK [13]. Since TTO has been thought to be close to the classical spin ice, the low-temperature dynamical behavior of TTO could be attributed to QSI [14]. Inspired by this intriguing idea, many experimental studies of TTO have been performed to date [15–20] (and references in Refs. [9, 21]). However the interpretation of experimental data has been a conundrum [9, 21], partly owing to strong sample dependence [15, 16, 22]. Among these studies, our investigation [16] of polycrystalline  $\text{Tb}_{2+x}\text{Ti}_{2-x}\text{O}_{7+y}$  showed that a very small change of  $x$  induces a quantum phase transition between a spin-liquid

state ( $x < -0.0025 = x_c$ ) and a LRO state with a hidden order parameter ( $x_c < x$ ). It is important to clarify the origin of this order parameter, which becomes dynamical in the spin-liquid state ( $x < x_c$ ).

In this and companion [23, 24] work, we try to reformulate the problem of TTO and to reinterpret its puzzling experimental data based on the theoretically predicted [25] electronic superexchange interactions. A novel ingredient of these interactions is the Onoda-type coupling [25] between neighboring electric quadrupole moments of non-Kramers  $\text{Tb}^{3+}$  ions. The theory [25] proposes an effective pseudospin-1/2 Hamiltonian described by the Pauli matrices representing both magnetic-dipole and electric-quadrupole moments. Depending on the parameters of the Hamiltonian there are two electric quadrupole ordering phases, which are candidates for the hidden order of TTO. These electric quadrupolar orders do not bring about observable magnetic Bragg peaks. However, these orders can be detected by their elementary excitations (inelastic magnetic scattering), and by proper interpretation using a linear spin-wave theory.

In this paper, starting from the crystal-field (CF) ground state doublet of TTO, we account for its single-site electric quadrupole moments, their LRO, and pseudospin wave excitations in the electric quadrupole LRO. A standard linear spin-wave theory predicts that the pseudospin wave in the electric quadrupole LRO is, in reality, a composite wave of magnetic-dipole and electric-quadrupole moments. We discuss this possibility for  $\text{Tb}_{2+x}\text{Ti}_{2-x}\text{O}_{7+y}$  using previously observed [16] low-energy magnetic excitation spectra of a polycrystalline sample with  $x = 0.005$  ( $T_c = 0.5$  K).

## II. CRYSTAL FIELD AND ELECTRIC MULTIPOLE MOMENT

The CF states and inelastic neutron excitation spectra of TTO have been investigated by many authors [26–30]; readers are referred to Ref. [30] for details. In a low

energy range, there are four CF states: ground doublet states and first-excited doublet states at  $E \sim 16$  K. Since the interesting temperature range is below 1 K, we neglect the first-excited doublet states and consider only the ground state doublet, for simplicity.

Among studies of CF, we adopt the CF parameters of Ref. [27] (or Ref. [28]). The CF ground state doublet of TTO can be written by

$$|\pm 1\rangle_D = A|\mp 4\rangle \pm B|\mp 1\rangle + C|\pm 2\rangle \mp D|\pm 5\rangle, \quad (1)$$

where  $|m\rangle$  stands for the  $|J=6, m\rangle$  state within a  $JLS$ -multiplet [31]. The coefficients [27] of Eq. (1) are  $A = 0.9581$ ,  $B = 0.1284$ ,  $C = 0.1210$ ,  $D = 0.2256$ . The local symmetry axes [25, 28] of the crystallographic four sites are

$$\mathbf{x}_0 = \frac{1}{\sqrt{6}}(1, 1, \bar{2}), \mathbf{y}_0 = \frac{1}{\sqrt{2}}(\bar{1}, 1, 0), \mathbf{z}_0 = \frac{1}{\sqrt{3}}(1, 1, 1) \quad (2)$$

for sites at  $\mathbf{t}_n + \mathbf{d}_0$  with  $\mathbf{d}_0 = \frac{1}{4}(0, 0, 0)$ ,

$$\mathbf{x}_1 = \frac{1}{\sqrt{6}}(1, \bar{1}, 2), \mathbf{y}_1 = \frac{1}{\sqrt{2}}(\bar{1}, \bar{1}, 0), \mathbf{z}_1 = \frac{1}{\sqrt{3}}(1, \bar{1}, \bar{1}) \quad (3)$$

for sites at  $\mathbf{t}_n + \mathbf{d}_1$  with  $\mathbf{d}_1 = \frac{1}{4}(0, 1, 1)$ ,

$$\mathbf{x}_2 = \frac{1}{\sqrt{6}}(\bar{1}, 1, 2), \mathbf{y}_2 = \frac{1}{\sqrt{2}}(1, 1, 0), \mathbf{z}_2 = \frac{1}{\sqrt{3}}(\bar{1}, 1, \bar{1}) \quad (4)$$

for sites at  $\mathbf{t}_n + \mathbf{d}_2$  with  $\mathbf{d}_2 = \frac{1}{4}(1, 0, 1)$ ,

$$\mathbf{x}_3 = \frac{1}{\sqrt{6}}(\bar{1}, \bar{1}, \bar{2}), \mathbf{y}_3 = \frac{1}{\sqrt{2}}(1, \bar{1}, 0), \mathbf{z}_3 = \frac{1}{\sqrt{3}}(\bar{1}, \bar{1}, 1) \quad (5)$$

for sites at  $\mathbf{t}_n + \mathbf{d}_3$  with  $\mathbf{d}_3 = \frac{1}{4}(1, 1, 0)$ , where  $\mathbf{t}_n$  is an FCC translation vector.

In the CF ground state doublet of Eq. (1), the magnetic-dipole and electric-multipole moment operators [32] are represented by  $2 \times 2$  matrices: the Pauli matrices  $\sigma^x$ ,  $\sigma^y$ ,  $\sigma^z$  and the unit matrix. The magnetic dipole moment operators within  $|\pm 1\rangle_D$  are

$$\begin{aligned} J_x = J_y = 0, \\ J_z = -(4A^2 + B^2 - 2C^2 - 5D^2)\sigma^z = -3.40\sigma^z, \end{aligned} \quad (6)$$

which implies that  $\text{Tb}^{3+}$  magnetic dipole moments behave as Ising-like spins.

As pointed out in Ref. [25], for non-Kramers ions in the pyrochlore structure including  $\text{Tb}^{3+}$  in TTO the CF ground doublet states have additionally electric multipole moments. These electric multipole moment operators are represented by  $\sigma^x$ ,  $\sigma^y$ , and the unit matrix. Using the explicit form of Eq. (1), the electric quadrupole moment

operators [32] within  $|\pm 1\rangle_D$  are expressed by

$$\begin{aligned} \frac{1}{2}[3J_z^2 - J(J+1)] &= 3A^2 - \frac{39}{2}B^2 - 15C^2 + \frac{33}{2}D^2 \\ &= 3.05, \\ \frac{\sqrt{3}}{2}[J_x^2 - J_y^2] &= \left(-\frac{21\sqrt{3}}{2}B^2 + 9\sqrt{10}AC\right)\sigma^x \\ &= 3.00\sigma^x, \\ \frac{\sqrt{3}}{2}[J_xJ_y + J_yJ_x] &= -\left(-\frac{21\sqrt{3}}{2}B^2 + 9\sqrt{10}AC\right)\sigma^y \\ &= -3.00\sigma^y, \\ \frac{\sqrt{3}}{2}[J_zJ_x + J_xJ_z] &= -\left(3\sqrt{30}BC + 9\sqrt{\frac{33}{2}}AD\right)\sigma^x \\ &= -8.16\sigma^x, \\ \frac{\sqrt{3}}{2}[J_yJ_z + J_zJ_y] &= -\left(3\sqrt{30}BC + 9\sqrt{\frac{33}{2}}AD\right)\sigma^y \\ &= -8.16\sigma^y. \end{aligned} \quad (7)$$

Similarly we can show that the electric 16-pole and 64-pole moment operators [32], expressed by the Racah operators [31]  $\tilde{O}_{p,q}(\mathbf{J})$  with  $p = 4$  and 6, respectively (or Stevens's operators), are proportional to  $\sigma^x \pm i\sigma^y$  or the unit matrix within  $|\pm 1\rangle_D$ . Therefore within the CF ground state doublet, pseudospin operators  $\sigma^x$  and  $\sigma^y$  represent the electric multipole moments. A single-site CF ground state expressed by

$$|\psi\rangle = (|1\rangle_D, |-1\rangle_D)\chi, \quad (8)$$

where  $\chi$  is the pseudospin wave-function, has the largest expectation of the magnetic dipole moment  $|\langle\psi|\sigma^z|\psi\rangle| = 1$  (and  $\langle\psi|\sigma^x|\psi\rangle = \langle\psi|\sigma^y|\psi\rangle = 0$ ) for  $\chi = \begin{pmatrix} 1 \\ 0 \end{pmatrix}$  or  $\chi = \begin{pmatrix} 0 \\ 1 \end{pmatrix}$ . The other states expressed by

$$\chi = \begin{pmatrix} \cos\frac{\theta}{2}e^{-i\phi/2} \\ \sin\frac{\theta}{2}e^{i\phi/2} \end{pmatrix} \quad (9)$$

in which  $\theta$  is in the range  $0 < \theta < \pi$  have finite expectation values of the electric quadrupole moment operators;  $\langle\psi|\sigma^x|\psi\rangle \neq 0$  and/or  $\langle\psi|\sigma^y|\psi\rangle \neq 0$ . These states have slightly deformed  $f$ -electron charge densities from that of the magnetic states with  $\theta = 0$  or  $\theta = \pi$ . More specifically, the approximate  $f$ -electron charge density [32] of the state  $|\psi\rangle$  is given by

$$\langle\psi|\rho(\mathbf{r})|\psi\rangle \simeq (-e)[R_f(r)]^2\langle\psi|\rho_e(\hat{\mathbf{r}})|\psi\rangle\frac{1}{4\pi}. \quad (10)$$

The angular dependence [32]  $\rho_e(\hat{\mathbf{r}})$  of this equation is

$$\rho_e(\hat{\mathbf{r}}) = n + \sum_{p=2,4,6;q} [4\pi(2p+1)]^{1/2}\alpha_p Y_{p,q}(\hat{\mathbf{r}})^* \tilde{O}_{p,q}(\mathbf{J}), \quad (11)$$

where  $(\alpha_2, \alpha_4, \alpha_6) = (\alpha, \beta, \gamma)$  are the Stevens factors [31],  $n = 8$  is the number of  $f$ -electrons, and  $Y_{p,q}(\hat{\mathbf{r}})$  are the spherical harmonics. By evaluating  $\langle\psi|\rho_e(\hat{\mathbf{r}})|\psi\rangle$  using several spinors of Eq. (9), one can show that the deformation of the  $f$ -electron charge density is mainly determined by the electric quadrupole moments. The electric

16-pole and 64-pole moments have non-negligible contributions to the deformation similarly to the analyses of the CF states [26–30]. In these meanings, the CF ground (pseudospin-1/2) states  $|\psi\rangle$  can be referred to as composite spin and quadrupole states.

### III. EFFECTIVE PSEUDOSPIN-1/2 HAMILTONIAN

The generic form of the effective pseudospin-1/2 Hamiltonian for non-Kramers CF ground state doublets of  $4f$  magnetic ions in the pyrochlore structure was derived in Ref. [25] by calculating the nearest-neighbor (NN) superexchange interaction. This Hamiltonian consists of two parts. The first part is the NN magnetic interaction

$$H_{\text{m,NN}} = J_{\text{nn}} \sum_{\langle \mathbf{r}, \mathbf{r}' \rangle} \sigma_{\mathbf{r}}^z \sigma_{\mathbf{r}'}^z, \quad (12)$$

which represents the NN classical spin-ice model for  $J_{\text{nn}} > 0$ . The second part is the NN quadrupolar interaction

$$H_{\text{q}} = J_{\text{nn}} \sum_{\langle \mathbf{r}, \mathbf{r}' \rangle} [2\delta(\sigma_{\mathbf{r}}^+ \sigma_{\mathbf{r}'}^- + \sigma_{\mathbf{r}}^- \sigma_{\mathbf{r}'}^+) + 2q(e^{2i\phi_{\mathbf{r},\mathbf{r}'}} \sigma_{\mathbf{r}}^+ \sigma_{\mathbf{r}'}^+ + \text{H.c.})], \quad (13)$$

where  $\sigma_{\mathbf{r}}^{\pm} = (\sigma_{\mathbf{r}}^x \pm i\sigma_{\mathbf{r}}^y)/2$  and  $\sigma_{\mathbf{r}}^{\alpha}$  ( $\alpha = x, y, z$  defined using the local axes Eqs. (2)-(5)) stand for the Pauli matrices of the pseudospin at a site  $\mathbf{r}$ . The phases  $\phi_{\mathbf{r},\mathbf{r}'}$  are  $\phi_{\mathbf{r},\mathbf{r}'} = 0, -2\pi/3$ , and  $2\pi/3$  for  $(i, i') = (0, 3), (1, 2), (i, i') = (0, 1), (2, 3)$ , and  $(i, i') = (0, 2), (1, 3)$ , respectively, where  $(\mathbf{r}, \mathbf{r}') = (\mathbf{t}_n + \mathbf{d}_i, \mathbf{t}_{n'} + \mathbf{d}_{i'})$ .

For the magnetic interaction of TTO we probably have to include the classical dipolar interaction, i.e.,

$$H_{\text{m}} = H_{\text{m,NN}} + Dr_{\text{nn}}^3 \sum_{\langle \mathbf{r}, \mathbf{r}' \rangle} \left\{ \frac{\mathbf{z}_{\mathbf{r}} \cdot \mathbf{z}_{\mathbf{r}'}}{|\Delta \mathbf{r}|^3} - \frac{3[\mathbf{z}_{\mathbf{r}} \cdot \Delta \mathbf{r}][\mathbf{z}_{\mathbf{r}'} \cdot \Delta \mathbf{r}]}{|\Delta \mathbf{r}|^5} \right\} \sigma_{\mathbf{r}}^z \sigma_{\mathbf{r}'}^z, \quad (14)$$

where the summation runs over all pairs of sites,  $r_{\text{nn}}$  is the NN distance, and  $\Delta \mathbf{r} = \mathbf{r} - \mathbf{r}'$ . The parameter  $D$  is determined by the magnetic moment of the CF ground state doublet. We adopt  $D = 0.29$  K, corresponding to the experimental value of the magnetic moment  $4.6 \mu_{\text{B}}$  [23]. As discussed in Refs. [33, 34], when the magnetic interaction of Eq. (14) represents the dipolar spin ice ( $J_{\text{nn}} + D_{\text{nn}} > 0$ ),  $H_{\text{m}}$  can be approximated by the NN classical spin-ice Hamiltonian [33]

$$H_{\text{m}} \simeq (J_{\text{nn}} + D_{\text{nn}}) \sum_{\langle \mathbf{r}, \mathbf{r}' \rangle} \sigma_{\mathbf{r}}^z \sigma_{\mathbf{r}'}^z, \quad (15)$$

where  $D_{\text{nn}} = \frac{5}{3}D = 0.48$  K.

In our computations we used an effective pseudospin-1/2 Hamiltonian of the form

$$H_{\text{eff}} = H_{\text{m}} + H_{\text{q}}. \quad (16)$$

We note that this is not very different from the original Onoda-type interaction [25] ( $D_{\text{nn}} = 0$ ) and results of Refs. [7, 25] can be approximately used at least in the electric quadrupolar phases, in which  $xy$ -components of the pseudospin ( $\sigma_{\mathbf{r}}^x, \sigma_{\mathbf{r}}^y$ ) show LRO and semi-classical theoretical treatments are applicable.

### IV. PSEUDOPIN WAVE

The studies [7, 23, 25] of the effective Hamiltonian of Eq. (16) showed that there are two electric quadrupolar states: the PAF state (planar antiferropseudospin) and the PF state (planar ferropseudospin) depending on the two parameters ( $\delta, q$ ) (see Fig. 7 in Ref. [25] and Fig. 3 in Ref. [7] for details). In these states, the  $xy$ -components of the pseudospin show LRO with the modulation vector  $\mathbf{k} = 0$ . It should be noted that this wave vector  $\mathbf{k} = 0$  is selected by quantum [7] and thermal [23, 25] fluctuations for PAF, i.e., by an order-by-disorder mechanism.

In order to calculate elementary excitations in the PAF and PF states, we choose one of the pseudospin structures

$$\langle \langle \sigma_{\mathbf{t}_n + \mathbf{d}_i}^x, \sigma_{\mathbf{t}_n + \mathbf{d}_i}^y \rangle \rangle = \begin{cases} (0, \langle \sigma^y \rangle) & (i = 0, 3) \\ -(0, \langle \sigma^y \rangle) & (i = 1, 2) \text{ (PAF)} \end{cases} \quad (17)$$

and

$$\langle \langle \sigma_{\mathbf{t}_n + \mathbf{d}_i}^x, \sigma_{\mathbf{t}_n + \mathbf{d}_i}^y \rangle \rangle = (0, \langle \sigma^y \rangle) \quad (i = 0, 1, 2, 3) \text{ (PF)}. \quad (18)$$

We apply the simple linear spin-wave theory, MF-RPA [31] (mean field, random phase approximation), in the same way as described in §3.5.2 of Ref. [31]. In MF-RPA,  $\langle \sigma^y \rangle$  of Eqs. (17) and (18) is calculated by the MF approximation. For the present purpose, we are interested in elementary excitations only at low temperatures, and  $\langle \sigma^y \rangle = 1$  is a good approximation. To obtain dispersion relations of pseudospin waves, MF-RPA utilizes the generalized susceptibility  $\chi(\mathbf{k}, E)$  and neutron magnetic scattering intensity  $S(\mathbf{Q}, E)$  [31]. Useful examples of MF-RPA computations including straightforward technical extensions for pyrochlore structures are described Refs. [35, 36]. General computational treatments of MF-RPA are discussed in Refs. [37, 38]. Following these references [31, 35, 36, 38], the generalized susceptibility is given by

$$\chi(\mathbf{k}, E) = [1 - \chi^0(E)J(\mathbf{k})]^{-1} \chi^0(E). \quad (19)$$

where  $\mathbf{k}$  is a wave vector in the first Brillouin zone,  $\chi^0(E)$  and  $J(\mathbf{k})$  denote the single-site generalized-susceptibility of the MF Hamiltonian and the Fourier transform of the exchange and dipolar coupling constants. The neutron magnetic scattering intensity  $S(\mathbf{Q} = \mathbf{G} + \mathbf{k}, E)$  is given

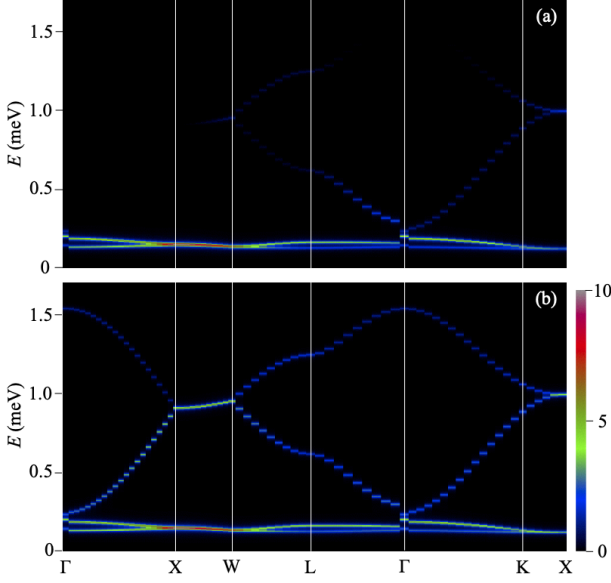


FIG. 1. Magnetic  $S(\mathbf{Q}, E)$  (a) and virtual  $S_v(\mathbf{Q}, E)$  (b) of the PAF ordering (Eq. (17)) using interaction parameters  $J_{\text{nn}} = 1$  K,  $q = 0.85$ , and  $\delta = 0$ .

by

$$S(\mathbf{Q}, E) \propto \frac{1}{1 - e^{-\beta E}} \sum_{\rho, \sigma} (\delta_{\rho, \sigma} - \hat{Q}_\rho \hat{Q}_\sigma) \times \sum_{i, i'} U_{\rho, z}^{(i)} U_{\sigma, z}^{(i')} \text{Im} \left\{ \chi_{i, z; i', z}(\mathbf{k}, E) e^{-i\mathbf{G} \cdot (\mathbf{d}_i - \mathbf{d}_{i'})} \right\}, \quad (20)$$

where only the local  $z$ -component of the pseudospin  $\sigma_{\mathbf{r}}^z$  contribute to the scattering. If one assumes that all the pseudospin components represent a magnetic dipole moment vector with an isotropic  $g$ -factor, virtual neutron scattering intensity  $S_v(\mathbf{Q}, E)$  is given by

$$S_v(\mathbf{Q}, E) \propto \frac{1}{1 - e^{-\beta E}} \sum_{\rho, \sigma} (\delta_{\rho, \sigma} - \hat{Q}_\rho \hat{Q}_\sigma) \times \sum_{i, \alpha, i', \alpha'} U_{\rho, \alpha}^{(i)} U_{\sigma, \alpha'}^{(i')} \text{Im} \left\{ \chi_{i, \alpha; i', \alpha'}(\mathbf{k}, E) e^{-i\mathbf{G} \cdot (\mathbf{d}_i - \mathbf{d}_{i'})} \right\}, \quad (21)$$

where  $U_{\rho, \alpha}^{(i)}$  is the rotation matrix [35, 36] from the local ( $\alpha$ ) frame defined at the sites  $\mathbf{t}_n + \mathbf{d}_i$  to the global ( $\rho$ ) frame.  $S_v(\mathbf{Q}, E)$  is useful when displaying dispersion relations of all pseudospin waves, because the amplitude of the electric quadrupole moment are excluded for  $S(\mathbf{Q}, E)$ .

In Fig. 1(a) we show the inelastic magnetic scattering intensity  $S(\mathbf{Q}, E)$  (Eq. (20)) of the the PAF ordering (Eq. (17)) along several symmetry directions in the FCC Brillouin zone using the interaction parameters  $J_{\text{nn}} = 1$  K,  $q = 0.85$ , and  $\delta = 0$  adopted in Ref. [23]. One can see two flat excitation branches in Fig. 1(a). We also show the virtual  $S_v(\mathbf{Q}, E)$  (Eq. (21)) in Fig. 1(b). This figure clearly shows that there are four excitation branches consistent with the  $\mathbf{k} = 0$  structure possessing

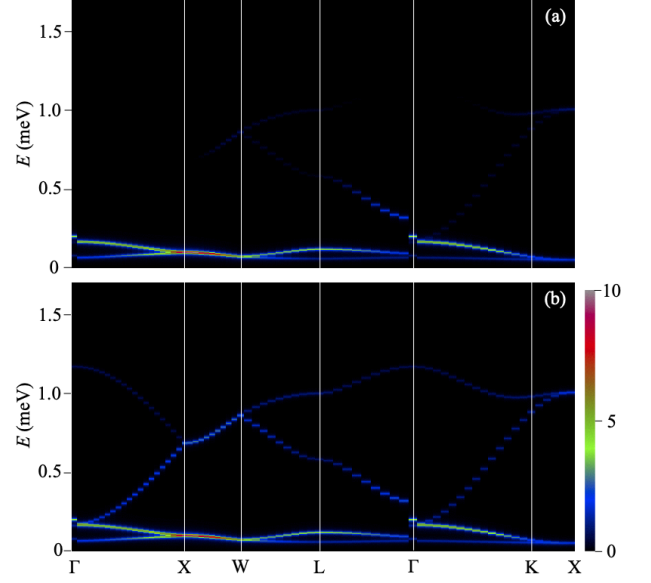


FIG. 2. Magnetic  $S(\mathbf{Q}, E)$  (a) and virtual  $S_v(\mathbf{Q}, E)$  (b) of the PAF ordering (Eq. (17)) using interaction parameters  $J_{\text{nn}} = 1$  K,  $q = 0.5$ , and  $\delta = 0.6$ .

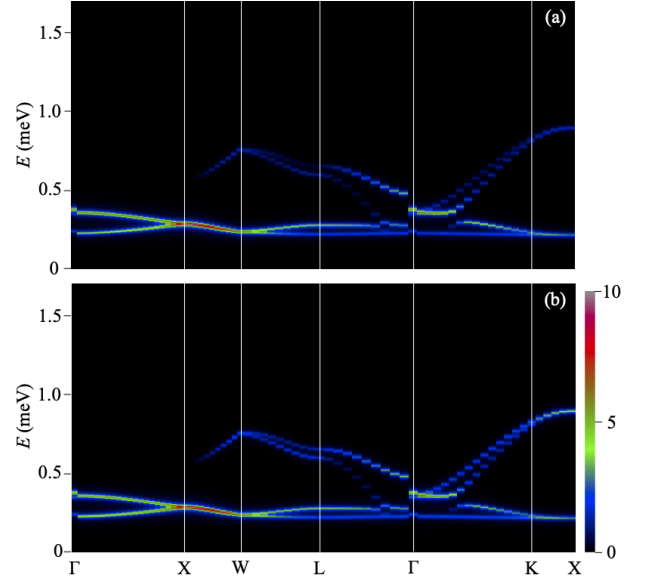


FIG. 3. Magnetic  $S(\mathbf{Q}, E)$  (a) and virtual  $S_v(\mathbf{Q}, E)$  (b) of the PF ordering (Eq. (18)) using interaction parameters  $J_{\text{nn}} = 1$  K,  $q = 0.8$ , and  $\delta = -0.6$ .

four sites in the unit cell. These four pseudospin-wave branches are composite spin ( $\sigma_{\mathbf{r}}^z$ ) and quadrupole ( $\sigma_{\mathbf{r}}^x$ ) waves. Figs. 1(a) and (b) show that the amplitude of the spin components is strong and weak in the two lower- $E$  and the two higher- $E$  branches, respectively. Fig. 2 shows the magnetic  $S(\mathbf{Q}, E)$  and virtual  $S_v(\mathbf{Q}, E)$  using different parameters  $J_{\text{nn}} = 1$  K,  $q = 0.5$ , and  $\delta = 0.6$  in the PAF phase (Eq. (17)). The two lower- $E$  excitation branches become more dispersive by the finite value of  $\delta$  compared to Fig. 1.

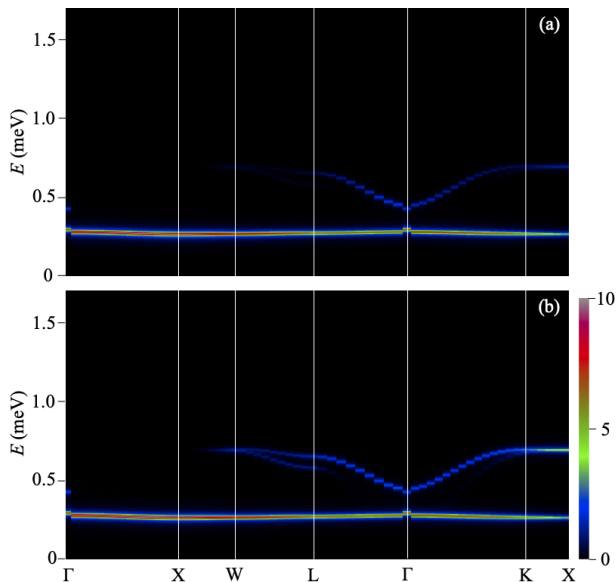


FIG. 4. Magnetic  $S(\mathbf{Q}, E)$  (a) and virtual  $S_v(\mathbf{Q}, E)$  (b) of the PF ordering (Eq. (18)) using interaction parameters  $J_{nn} = 1$  K,  $q = 0$ , and  $\delta = -0.6$ .

In Fig. 3 we show the magnetic  $S(\mathbf{Q}, E)$  and virtual  $S_v(\mathbf{Q}, E)$  using parameters  $J_{nn} = 1$  K,  $q = 0.8$ , and  $\delta = -0.6$ , which are in the PF phase (Eq. (18)). Compared to the PAF cases, the difference between the magnetic and virtual  $S(\mathbf{Q}, E)$  becomes less pronounced. Fig. 4 shows the magnetic  $S(\mathbf{Q}, E)$  and virtual  $S_v(\mathbf{Q}, E)$  using parameters  $J_{nn} = 1$  K,  $q = 0$ , and  $\delta = -0.6$  in the PF phase (Eq. (18)). For vanishing  $q = 0$ , the two lower- $E$  branches are more flattened and merge into almost one branch.

## V. MAGNETIC SPECTRA OF POLYCRYSTALLINE $\text{Tb}_{2+x}\text{Ti}_{2-x}\text{O}_{7+y}$

Finally, we would like to compare the previously observed [16] inelastic magnetic neutron scattering spectra peaked around  $E = 0.1$  meV with the present pseudospin wave calculation. The sample is the polycrystalline  $\text{Tb}_{2+x}\text{Ti}_{2-x}\text{O}_{7+y}$  with  $x = 0.005$  ( $T_c = 0.5$  K) [16]. The neutron scattering experiment was performed on the time-of-flight spectrometer ILL-IN5 operated with  $\lambda = 10$  Å. Fig. 5(b) shows  $Q$ -dependent powder spectra taken at  $T = 0.1$  K. These data should be compared with powder averaging of the magnetic  $S(\mathbf{Q}, E)$ . Fig. 5(a) shows an example of this powder averaged  $S(|\mathbf{Q}|, E)$  choosing the parameters  $J_{nn} = 1$  K,  $q = 0.8$ , and  $\delta = 0$ , which are in the PAF phase (Eq. (17)). We think that these figures show reasonably good agreement between the calculation and the observation. In spite of using the over-simplified model Hamiltonian for TTO and the crude linear-spin-wave theory for the frustrated quantum system, essential features of experimental spectra can be reproduced by the approximate calculation. The

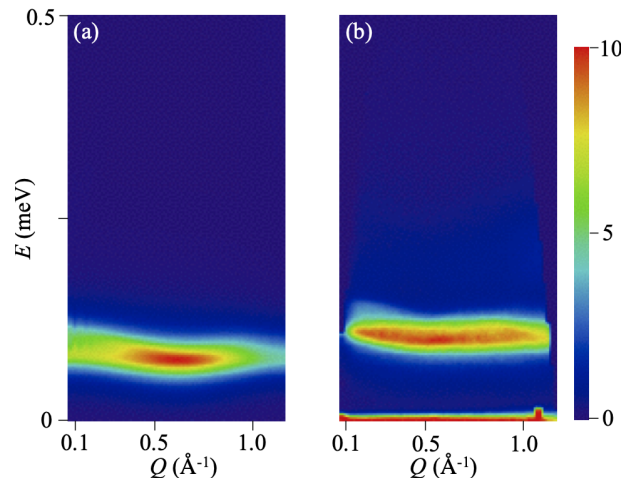


FIG. 5. (a) Powder averaged magnetic  $S(|\mathbf{Q}|, E)$  of the PAF ordering (Eq. (17)) using interaction parameters  $J_{nn} = 1$  K,  $q = 0.8$ , and  $\delta = 0$ . (b) Inelastic neutron scattering spectra of polycrystalline  $\text{Tb}_{2+x}\text{Ti}_{2-x}\text{O}_{7+y}$  with  $x = 0.005$  at  $T = 0.1$  K well below  $T_c$ .

slight  $Q$ -dependence and the non-resolution limited peak-width,  $\Delta E \gg (\Delta E)_{\text{resolution}} = 0.01$  meV, have been one of the puzzling observations of TTO. The present interpretation using the composite spin-quadrupole wave can be an answer [23, 24].

## VI. SUMMARY

In this study, we try to reformulate the problem of  $\text{Tb}_{2+x}\text{Ti}_{2-x}\text{O}_{7+y}$  and reinterpret its puzzling experimental facts based on the theoretically predicted [25] pseudospin-1/2 Hamiltonian including the electronic superexchange interaction between electric quadrupole moments. In this scenario, the hidden order in some TTO samples is an electric quadrupolar LRO. Although this LRO does not give rise to strong magnetic Bragg scattering, it can be observed by inelastic magnetic neutron scattering as a composite spin-quadrupole wave. We employ a MF-RPA linear spin-wave theory and compare its computation with previously observed low-energy magnetic excitation spectra of a polycrystalline sample with  $x = 0.005$  ( $T_c = 0.5$  K). Quite intriguingly, the interaction parameters used in Fig. 5(a) are located very close to the phase boundary between the PAF and U(1) quantum spin-liquid states [7, 23, 25]. This may possibly imply that  $\text{Tb}_{2+x}\text{Ti}_{2-x}\text{O}_{7+y}$  samples with  $x < x_c$  are in the U(1) quantum spin-liquid phase [23].

## ACKNOWLEDGMENTS

We thank S. Onoda and Y. Kato for useful discussions. This work was supported by JSPS KAKENHI grant numbers 25400345 and 26400336. The neutron scattering

performed using ILL-IN5 (France) was transferred from

JRR3-HER (proposal 11567) with the approval of ISSP, Univ. of Tokyo, and JAEA, Tokai, Japan.

- 
- [1] C. Lacroix, P. Mendels, and F. Mila, eds., *Introduction to Frustrated Magnetism* (Springer, Berlin, Heidelberg, 2011).
- [2] J. S. Gardner, M. J. P. Gingras, and J. E. Greedan, Magnetic pyrochlore oxides, *Rev. Mod. Phys.* **82**, 53 (2010).
- [3] S. T. Bramwell and M. J. P. Gingras, *Science* **294**, 1495 (2001).
- [4] C. Castelnovo, R. Moessner, and S. L. Sondhi, Magnetic monopoles in spin ice, *Nature* **451**, 42 (2008).
- [5] M. Hermele, M. P. A. Fisher, and L. Balents, Pyrochlore photons: The  $U(1)$  spin liquid in a  $S = \frac{1}{2}$  three-dimensional frustrated magnet, *Phys. Rev. B* **69**, 064404 (2004).
- [6] L. Savary and L. Balents, Coulombic Quantum Liquids in Spin-1/2 Pyrochlores, *Phys. Rev. Lett.* **108**, 037202 (2012).
- [7] S. Lee, S. Onoda, and L. Balents, Generic quantum spin ice, *Phys. Rev. B* **86**, 104412 (2012).
- [8] Y. Kato and S. Onoda, Numerical evidence of quantum melting of spin ice: Quantum-to-classical crossover, *Phys. Rev. Lett.* **115**, 077202 (2015).
- [9] M. J. P. Gingras and P. A. McClarty, Quantum spin ice: a search for gapless quantum spin liquids in pyrochlore magnets, *Rep. Prog. Phys.* **77**, 056501 (2014).
- [10] O. Benton, O. Sikora, and N. Shannon, Seeing the light: Experimental signatures of emergent electromagnetism in a quantum spin ice, *Phys. Rev. B* **86**, 075154 (2012).
- [11] L.-J. Chang, S. Onoda, Y. Su, Y.-J. Kao, K.-D. Tsuei, Y. Yasui, K. Kakurai, and M. R. Lees, Higgs transition from a magnetic Coulomb liquid to a ferromagnet in  $\text{Yb}_2\text{Ti}_2\text{O}_7$ , *Nature Communications* **3**, 992 (2012).
- [12] K. A. Ross, L. Savary, B. D. Gaulin, and L. Balents, Quantum excitations in quantum spin ice, *Phys. Rev. X* **1**, 021002 (2011).
- [13] J. S. Gardner, S. R. Dunsiger, B. D. Gaulin, M. J. P. Gingras, J. E. Greedan, R. F. Kiefl, M. D. Lumsden, W. A. MacFarlane, N. P. Raju, J. E. Sonier, I. Swainson, and Z. Tun, Cooperative Paramagnetism in the Geometrically Frustrated Pyrochlore Antiferromagnet  $\text{Tb}_2\text{Ti}_2\text{O}_7$ , *Phys. Rev. Lett.* **82**, 1012 (1999).
- [14] H. R. Molavian, M. J. P. Gingras, and B. Canals, Dynamically Induced Frustration as a Route to a Quantum Spin Ice State in  $\text{Tb}_2\text{Ti}_2\text{O}_7$  via Virtual Crystal Field Excitations and Quantum Many-Body Effects, *Phys. Rev. Lett.* **98**, 157204 (2007).
- [15] H. Takatsu, H. Kadowaki, T. J. Sato, J. W. Lynn, Y. Tabata, T. Yamazaki, and K. Matsuhira, Quantum spin fluctuations in the spin-liquid state of  $\text{Tb}_2\text{Ti}_2\text{O}_7$ , *J. Phys. Condens. Matter* **24**, 052201 (2012).
- [16] T. Taniguchi, H. Kadowaki, H. Takatsu, B. Fåk, J. Ollivier, T. Yamazaki, T. J. Sato, H. Yoshizawa, Y. Shimura, T. Sakakibara, T. Hong, K. Goto, L. R. Yaraskavitch, and J. B. Kycia, Long-range order and spin-liquid states of polycrystalline  $\text{Tb}_{2+x}\text{Ti}_{2-x}\text{O}_{7+y}$ , *Phys. Rev. B* **87**, 060408 (2013).
- [17] S. Petit, P. Bonville, J. Robert, C. Decorse, and I. Mirebeau, Spin liquid correlations, anisotropic exchange, and symmetry breaking in  $\text{Tb}_2\text{Ti}_2\text{O}_7$ , *Phys. Rev. B* **86**, 174403 (2012).
- [18] T. Fennell, M. Kenzelmann, B. Roessli, H. Mutka, J. Ollivier, M. Ruminy, U. Stuhr, O. Zaharko, L. Bovo, A. Cervellino, M. K. Haas, and R. J. Cava, Magnetoelastic Excitations in the Pyrochlore Spin Liquid  $\text{Tb}_2\text{Ti}_2\text{O}_7$ , *Phys. Rev. Lett.* **112**, 017203 (2014).
- [19] K. Fritsch, K. A. Ross, Y. Qiu, J. R. D. Copley, T. Guidi, R. I. Bewley, H. A. Dabkowska, and B. D. Gaulin, Antiferromagnetic spin ice correlations at  $(\frac{1}{2}, \frac{1}{2}, \frac{1}{2})$  in the ground state of the pyrochlore magnet  $\text{Tb}_2\text{Ti}_2\text{O}_7$ , *Phys. Rev. B* **87**, 094410 (2013).
- [20] K. Fritsch, E. Kermarrec, K. A. Ross, Y. Qiu, J. R. D. Copley, D. Pomaranski, J. B. Kycia, H. A. Dabkowska, and B. D. Gaulin, Temperature and magnetic field dependence of spin-ice correlations in the pyrochlore magnet  $\text{Tb}_2\text{Ti}_2\text{O}_7$ , *Phys. Rev. B* **90**, 014429 (2014).
- [21] S. Petit, S. Guitteny, J. Robert, P. Bonville, C. Decorse, J. Ollivier, H. Mutka, and I. Mirebeau, Spin dynamics in highly frustrated pyrochlore magnets, *EPJ Web of Conferences* **83**, 03012 (2015).
- [22] Y. Chapuis, Ph.D. thesis, Université Joseph Fourier (2009), <http://tel.archives-ouvertes.fr/tel-00463643/en/>.
- [23] H. Takatsu, S. Kittaka, A. Kasahara, Y. Kono, T. Sakakibara, Y. Kato, S. Onoda, B. Fåk, J. Ollivier, J. W. Lynn, T. Taniguchi, M. Wakita, and H. Kadowaki, arXiv:1506.04545.
- [24] M. Wakita, T. Taniguchi, H. Edamoto, H. Takatsu, and H. Kadowaki, arXiv:1509.04583.
- [25] S. Onoda and Y. Tanaka, Quantum fluctuations in the effective pseudospin- $\frac{1}{2}$  model for magnetic pyrochlore oxides, *Phys. Rev. B* **83**, 094411 (2011).
- [26] M. J. P. Gingras, B. C. den Hertog, M. Faucher, J. S. Gardner, S. R. Dunsiger, L. J. Chang, B. D. Gaulin, N. P. Raju, and J. E. Greedan, Thermodynamic and single-ion properties of  $\text{Tb}^{3+}$  within the collective paramagnetic-spin liquid state of the frustrated pyrochlore antiferromagnet  $\text{Tb}_2\text{Ti}_2\text{O}_7$ , *Phys. Rev. B* **62**, 6496 (2000).
- [27] I. Mirebeau, P. Bonville, and M. Hennion, Magnetic excitations in  $\text{Tb}_2\text{Sn}_2\text{O}_7$  and  $\text{Tb}_2\text{Ti}_2\text{O}_7$  as measured by inelastic neutron scattering, *Phys. Rev. B* **76**, 184436 (2007).
- [28] A. Bertin, Y. Chapuis, P. Dalmas de Réotier, and A. Yaouanc, Crystal electric field in the  $\text{R}_2\text{Ti}_2\text{O}_7$  pyrochlore compounds, *J. Phys. Condens. Matter* **24**, 256003 (2012).
- [29] J. Zhang, K. Fritsch, Z. Hao, B. V. Bagheri, M. J. P. Gingras, G. E. Granroth, P. Jiramongkolchai, R. J. Cava, and B. D. Gaulin, Neutron spectroscopic study of crystal field excitations in  $\text{Tb}_2\text{Ti}_2\text{O}_7$  and  $\text{Tb}_2\text{Sn}_2\text{O}_7$ , *Phys. Rev. B* **89**, 134410 (2014).
- [30] A. J. Princep, H. C. Walker, D. T. Adroja, D. Prabhakaran, and A. T. Boothroyd, Crystal field states of  $\text{Tb}^{3+}$  in the pyrochlore spin liquid  $\text{Tb}_2\text{Ti}_2\text{O}_7$  from neutron spectroscopy, *Phys. Rev. B* **91**, 224430 (2015).
- [31] J. Jensen and A. R. Mackintosh, *Rare Earth Magnetism* (Clarendon Press, Oxford, 1991).

- [32] H. Kusunose, Description of Multipole in f-Electron Systems, *J. Phys. Soc. Jpn.* **77**, 064710 (2008).
- [33] B. C. den Hertog and M. J. P. Gingras, Dipolar interactions and origin of spin ice in ising pyrochlore magnets, *Phys. Rev. Lett.* **84**, 3430 (2000).
- [34] S. V. Isakov, R. Moessner, and S. L. Sondhi, Why spin ice obeys the ice rules, *Phys. Rev. Lett.* **95**, 217201 (2005).
- [35] Y.-J. Kao, M. Enjalran, A. Del Maestro, H. R. Molavian, and M. J. P. Gingras, Understanding paramagnetic spin correlations in the spin-liquid pyrochlore  $\text{Tb}_2\text{Ti}_2\text{O}_7$ , *Phys. Rev. B* **68**, 172407 (2003).
- [36] S. Petit, P. Bonville, I. Mirebeau, H. Mutka, and J. Robert, Spin dynamics in the ordered spin ice  $\text{Tb}_2\text{Sn}_2\text{O}_7$ , *Phys. Rev. B* **85**, 054428 (2012).
- [37] M. Rotter, High speed algorithm for the calculation of magnetic and orbital excitations in rare earth based systems, *Comput. Mater. Sci.* **38**, 400 (2006).
- [38] M. Rotter et al., Manual and references of McPhase, <http://www.mcphase.de/>.